Available online at www.sciencedirect.com
ScienceDirect
Trans. Nonferrous Met. Soc. China 25(2015) 30−35
Transactions of Nonferrous Metals Society of China
www.tnmsc.cn

Microstructure and properties of plasma remelted AZ91D magnesium alloy

Hong-zhi CUI, Zhao-tao MENG, Cheng-zhu XIAO, Jin-quan SUN, Cui-xiang WANG

School of Materials Science and Engineering, Shandong University of Science and Technology, Qingdao 266590, China

Received 3 January 2014; accepted 20 May 2014

Abstract: The surface of AZ91D magnesium alloy was remelted by plasma beam. The microstructure, composition, hardness, wear and corrosion resistance of the plasma remelted layer (PRL) were characterized. The results show that there is extremely fine and dendrite structure in the PRL at low magnification observation, which is still composed of α-Mg and β-$Mg_{17}Al_{12}$ phases. But at high magnification observation, the microstructure of the PRL is equiaxial crystalline grains with size of 3−5 μm. And also the content of α-Mg phase decreases while that of β-$Mg_{17}Al_{12}$ increases and distributes more uniformly in α-Mg matrix compared with the substrate. The hardness of the PRL is much higher than that of the substrate. There are plastic deformation, grains uprooting and tearing evidence with tiny even dimples in the tensile fracture of the PRL, which are different from the substrate. Furthermore, the surface wear and corrosion resistance of AZ91D are improved significantly after plasma remelting.

Key words: magnesium alloy; plasma remelting; solid solution strengthening; refined crystalline strengthening; wear resistance; corrosion resistance

1 Introduction

Magnesium alloys are applicable to automobile and aviation industry due to their low density, high specific strength and stiffness, and good shock absorption and noise reduction [1]. But their wide application is limited because of poor wear and corrosion resistance. It is difficult to improve the wear and corrosion resistance by alloying due to the segregation of alloying elements and formation of undesirable brittle intermetallic phases in magnesium alloy [2]. As most of the wear and corrosion damages start with the surface, it is very important to change the surface composition and microstructure of magnesium alloy. In order to improve the surface properties, a variety of surface modification technologies such as laser surface cladding [3−7], laser surface melting [8,9], micro-arc oxidation [10,11], metal plating [12], vapor deposition [13], organic coating [14], and chemical conversion coating [15,16] have been studied. Among them, laser surface melting and cladding are the most promising methods, as they can allow the formation of hard and dense protective coatings even at fast speed.

By making use of high energy laser, the surface of magnesium alloy could be melted or cladded quickly, the microstructure and properties can be improved significantly [17−19]. COY and VIEJO [20] found that by laser melting (LSM) the surface of die cast AZ91D alloy, a kind of homogeneous and refined microstructure was obtained, and the dissolution of a large amount of coarse intermetallic phases made the enrichment of aluminum in matrix greatly. Hence, the corrosion resistance especially localized corrosion resistance of AZ91D alloy was improved compared with the substrate. ZHANG et al [21] reported the wear behavior of AM50 magnesium alloy after LSM. They found that after laser melting, the microstructure became fine columnar dendrite. Although the wear friction coefficient curve was similar to that of the untreated AM50 substrate, the wear volume of the laser melted layer was decreased by 42%. Thus, the hardness and wear resistance of the laser melted layer were improved due to the grain refinement.

Plasma beam is a kind of compressed arc with high energy density and extremely high temperature. Compared with laser processing, plasma cladding is simpler and easier to operate. Furthermore, the cost of the plasma equipment is much lower than that of laser equipment [22].

Foundation item: Projects (51072104, 51272141) supported by the National Natural Science Foundation of China; Project (ts20110828) supported by the Taishan Scholars Project of Shandong Province, China; Project (2015AA034404) supported by the Ministry of Science and Technology of China
Corresponding author: Hong-zhi CUI; Tel: +86-532-86057929; E-mail: cuihongzhi1965@163.com
DOI: 10.1016/S1003-6326(15)63575-0

In this work, a kind of plasma remelted layer (PRL) on the surface of AZ91D was obtained by high energy density plasma beam. The microstructure, hardness, tensile fracture and wear and corrosion resistance were analysed, with intent of providing theoretical and experimental reference for improving the properties of magnesium alloys.

2 Experimental

The raw material used in this work was AZ91D. The device was DGR-5 atmospheric plasma apparatus with Ar as ionizating and protecting gas. AZ91D alloy plate was cut into samples with dimensions of 30 mm×30 mm×20 mm with line cutting machine. Then, the sheets were fixed to the working platform, and the surface was scanning remelted with plasma beam as shown in Fig. 1. The selected diameter and compression ratio of plasma generator nozzle for testing were 10 mm and 2, respectively, the distance between the nozzle and sample, i.e., the beam length was 10 mm, and the overlap ratio while scanning heating was 20%. All the parameters of the remelting process are listed in Table 1.

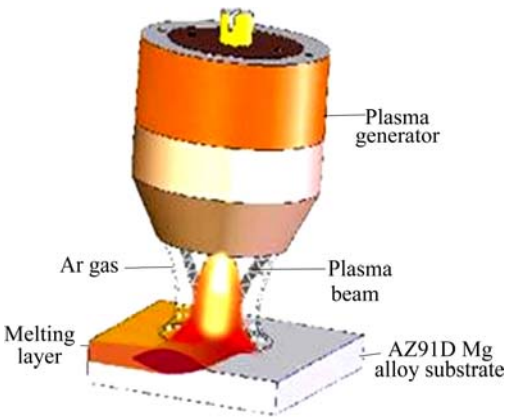

Fig. 1 Schematic illustration of plasma beam scanning remelting surface

The samples were characterized by X-ray diffraction (XRD, D/Max, Cu K_{α}, λ=1.542 Å, scanning speed of 0.02 (°)/s) to identify the crystalline phases. The polished and chemical etched samples were prepared for the analyses of microstructure and composition which were carried out on scanning electron microscope (SEM, KYKY2800B, voltage of 20 kV) and electron probe microanalysis (EPMA, JXA-8230, image current of 5×10^{-10} A, composition current of 5×10^{-8} A, voltage of 15 kV), respectively. The microhardnesses of different regions were measured by microhardness tester (FM-700, load of 100 N, 15 s). The tensile test was carried out on WDW-3100 electronic universal testing machine. The wear resistance was tested with M-2000 wear-test machine (load: 100 N; velocity: 200 r/min; time: 5 min). The anodic polarization of the melted layer and the raw AZ91D alloy was measured in 3.5% NaCl solution by using an electrochemical workstation (PARSTAT, 2273) at a scan rate of 1 mV/s. Three-electrode system was applied. The reference electrode was a saturated calomel electrode (SCE), and the counter electrode was a platinum electrode.

3 Results

3.1 Phase analysis

Figure 2 shows the XRD results of AZ91D PRL and substrate. It is obvious that after plasma remelting, the PRL is still composed of α-Mg and β-$Mg_{17}Al_{12}$ phases despite of the content of each phase changing. Figure 3 shows the ratio of I_{β}/I_{α} of the PRL with different electric currents. It indicates that I_{β}/I_{α} of the PRL is larger than that of the substrate. The larger the current is, the more the β-$Mg_{17}Al_{12}$ phase is. Because of the high temperature during the remelting process, some of Mg and Al elements may be burned or evaporated out in the molten bath due to the low melting point, and the loss rate of Mg is larger than that of Al. This may result in the formation of more β-$Mg_{17}Al_{12}$ phase in the PRL. As the energy density of the plasma beam increases with the current increasing the larger the current is, the more obvious this kind of phenomenon is.

3.2 Microstructure and element distribution analysis

Figure 4 shows the microstructures of the samples. Plasma melting results in grain refinement and the formation of fine dendrites as a result of the high speed heating and cooling, directional heat dissipating (Fig. 4(a)). At higher magnifying observation, the grains 3−5 μm in size and nearly dendrite shape as arrow *A* pointed in Fig. 4(a). Figure 4(b) shows the morphology of the cross-section which consists of two parts, the left part is PRL and the right part is near the substrate. The

Table 1 Parameters of plasma beam remelting process

Sample No.	Selected diameter/mm	Compression ratio	Beam length/mm	Overlap ratio/%	Scanning speed/($mm\cdot s^{-1}$)	Flow rate/ ($m^3\cdot h^{-1}$)	Current/A
1	10	2	10	20	2	0.2	45
2	10	2	10	20	2	0.2	55
3	10	2	10	20	2	0.2	65

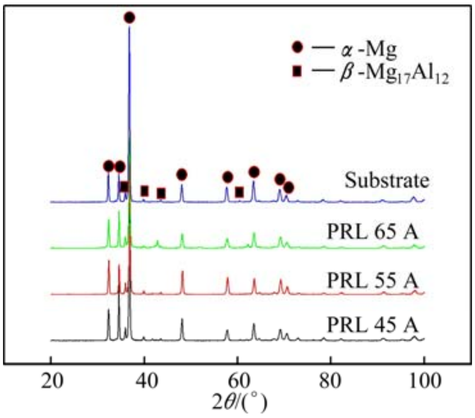

Fig. 2 XRD patterns of AZ91D PRL with different currents and substrate

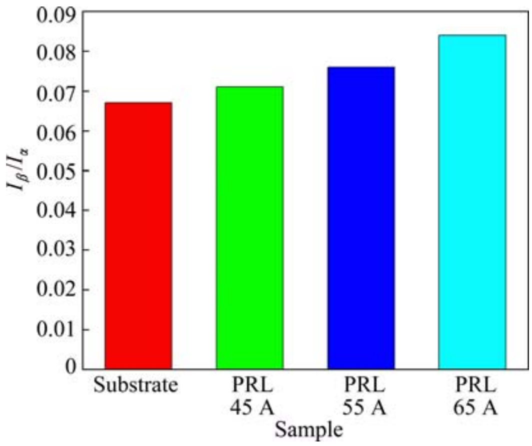

Fig. 3 Semi-quantitative analysis results of phases on AZ91D surface by plasma remelting

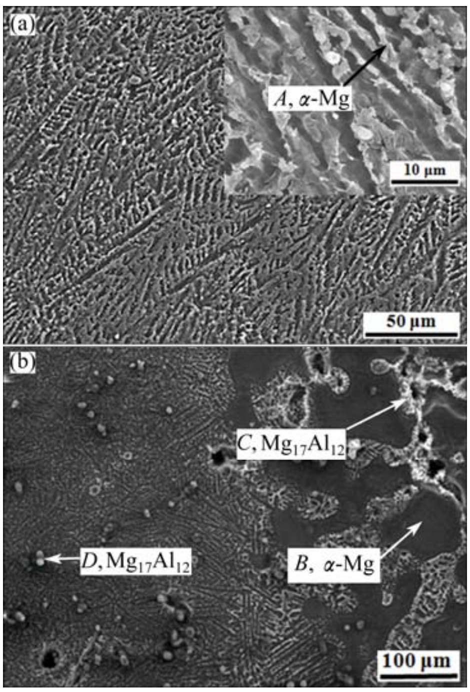

Fig. 4 SEM micrographs of PRL, transition zone and substrate with current of 55 A: (a) Surface of PRL; (b) Cross-section of PRL and substrate

grains of the substrate are coarse and irregular as arrow *B* pointed. There are some fish-bone shaped grains that distribute along the grains of the matrix as arrow *C* pointed, and there are also lots of white and fine round particles in both the coarse substrate and the fine dendrite layer as arrow *D* pointed. From the substrate to the PRL, the microstructure is quiet different, the coarse substrate and fish-bone morphology disappear instead of dendrites and white round particles (eutectic phases).

The composition analysis of Fig. 4 is given in Table 2. We can deduce that the fine dendritic phase in the PRL at point *A* in Fig. 4(a) is α-Mg, which is formed due to fast heating and cooling. And the coarse grain with equiaxial shape at point *B* near the substrate in Fig. 4(b) is also α-Mg, which represents the primary α-Mg phase, and the relative content of Al is less than that of fine dendritic phase, as point *A*. Points *C* and *D* which represent fish-bone shaped network and white round particles, respectively, as shown in Fig. 4(b), can be inferred as $Mg_{17}Al_{12}$ phase referring to their elements proportion, shapes and XRD results. During the fast heating process, the primary precipitated coarse α-Mg grains and most of the fish-bone network shaped β-$Mg_{17}Al_{12}$ grains on the matrix are melted and dissolved. And the remaining undissolved β-$Mg_{17}Al_{12}$ grains become round shape particles. During the fast cooling process, the liquid which is rich in aluminum forms fine dendritic α-Mg, due to fast directionally solidification.

Table 2 Quantitive analysis of points shown in Fig. 4

Point	Mass fraction/%		Mole fraction/%	
	Mg	Al	Mg	Al
A	82.45	17.55	84.09	15.91
B	87.32	12.68	88.57	11.43
C	65.36	34.64	67.98	32.02
D	61.74	38.26	64.48	35.52

3.3 Tensile fracture analysis

Both the plasma remelted and raw AZ91D alloy samples were subjected to a tensile test. The fracture morphologies are shown in Fig. 5. The fracture morphology in the PRL has plastic deformation evidence (Fig. 5(a)). At high magnification image, as shown in Fig. 5(b), it is obvious that the crystalline grains are equiaxial and the size is only 3−5 μm in accordance with Fig. 4(a). Given the total fracture surface of PRL is fine and homogeneous, and the existence of plastic deformation, obvious grains uprooting and tearing trace evidence with tiny evenly dimples, we can conclude that the fracture mode should be the integration of transgranular fracture, intergranular fracture and even ductile fracture.

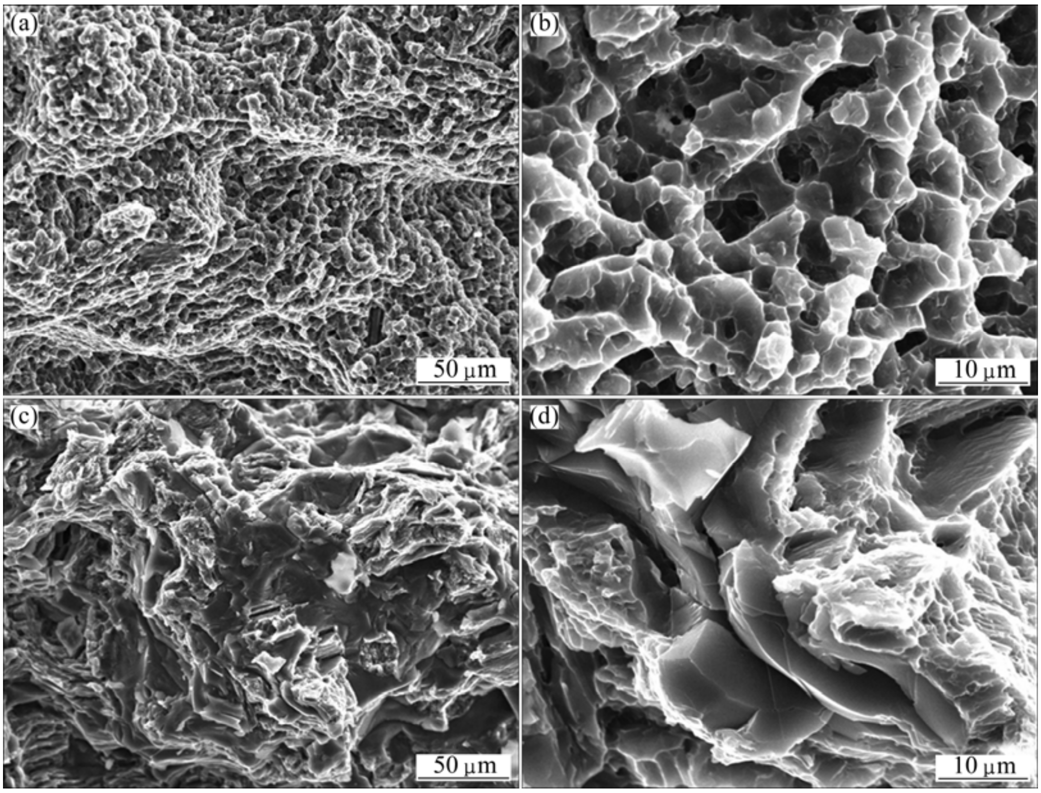

Fig. 5 SEM images of tensile fracture of PRL at remelting current of 55 A (a, b) and substrate (c, d)

But the fracture surface of raw AZ91D alloy (Figs. 5(c) and (d)), is much coarse and heterogeneous, and there are some level face and smooth cleavage morphology accompanied by some cracks, which indicates a kind of typical brittleness transgranular fracture mechanism.

3.4 Hardness

The microhardness of the PRL is shown in Fig. 6. The average hardness of the PRL is HV 105−125 which is much higher than that of substrate (HV 60−70). When the current increases, the energy density of the plasma beam is increased, so the depth of the PRL increases. With the increase of current from 45 A to 65 A, the depth of the PRL (microhardness >HV 90) increases from 1.0 mm to 2.5 mm.

3.5 Wear and corrosion resistance

The wear resistance of the PRL is improved obviously as shown in Fig. 7. When the current of plasma beam is 55 A or 65 A, the wear resistance of the PRL is almost twice as high as that of the raw AZ91D alloy, and the varying of current has no obvious effect on the wear resistance.

Figure 8 shows the potentiodynamic polarization curves of the PRL and raw AZ91D. Compared with the raw AZ91D, the J_{corr} of the PRL is reduced significantly, and φ_{corr} is increased by 50 mV. Therefore, after plasma

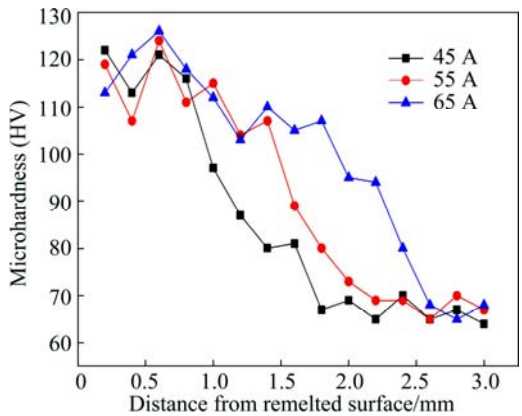

Fig. 6 Microhardness of PRL with different currents

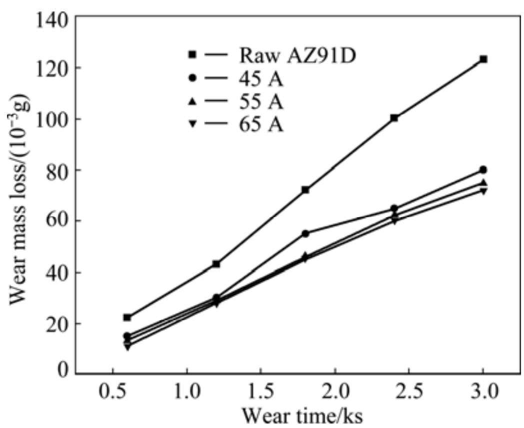

Fig. 7 Relationship between wear mass loss and wear time of PRL sample and AZ91D substrate

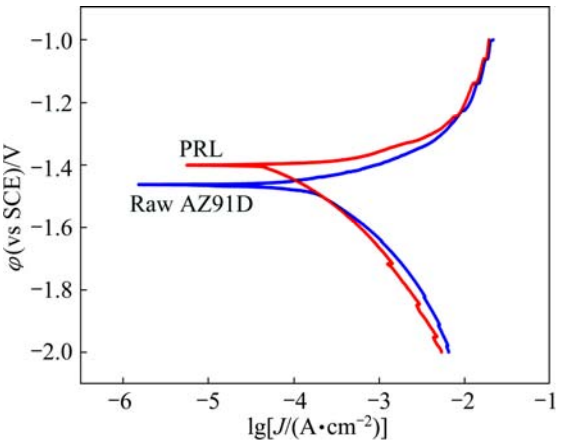

Fig. 8 Potentiodynamic polarization curves of PRL and raw AZ91D

remelting, both the wear resistance and corrosion resistance can be improved significantly.

4 Discussion

The PRL on the surface of AZ91D is obtained by high energy density plasma treatment. The microstructures of the PRL are refined to be fine column or dendritic shapes. According to the Hall-Petch equation [23,24]: $\sigma_s = \sigma_0 + Kd^{1/2}$, where σ_s is the yield strength; d is the average grain size; K and σ_0 are constants related to the material, the strength is easy to be influenced by the size of the grains. The grain refinement reduces the tendency of stress concentration, the cracks are difficult to produce and propagate. And if the cracks propagate, their directions have to change several times to consume more fracture energy. Therefore, it is helpful to reducing the brittleness and improving the strength and ductility of Mg alloy.

And also during the plasma remelting process, a large number of Al elements from the decomposition of $Mg_{17}Al_{12}$ are soluted into α-Mg in the heating process but not allowed to precipitate out as $Mg_{17}Al_{12}$ in the rapid cooling process. Thus, both solid solution strengthening and grain refining strengthening contribute to improving the hardness and strength of the PRL. Simultaneously, during the wear process, the wear debrises are small and thin and is not easy to rupture from the substrate. Thus, the mass loss rate of the PRL can be decreased and the wear resistance can be promoted.

Furthermore, a great deal of Al element solid soluted into α-Mg can promote the electrode potential of the PRL and form dense aluminum oxide films. And also the redistribution and homogenization of β-$Mg_{17}Al_{12}$ phase can decrease the effect of galvanic corrosion [17]. As a consequence, the corrosion resistance of the PRL is improved remarkably.

5 Conclusions

1) PRL on the surface of AZ91D is obtained by high energy density plasma beam treatment. The PRL is still composed of α-Mg and β-$Mg_{17}Al_{12}$. However, compared with the substrate, the content of α-Mg is increased, while the content of β-$Mg_{17}Al_{12}$ is decreased.

2) The microstructure of the PRL is greatly refined due to rapid heating and cooling. The tensile fracture morphology is fine and homogeneous with the fracture mode of integration of transgranular fracture, intergranular fracture and even ductile fracture.

3) The refined crystalline strengthening and solid solution strengthening of plasma remelting contribute greatly to improving the microhardness and wear resistance of the PRL. Furthermore, a large amount of Al elements are solid soluted into α-Mg and form dense aluminum oxide films, and also the redistribution and homogenization of β-$Mg_{17}Al_{12}$ phase promote the corrosion resistance remarkably.

References

[1] YANG Z, LI J P, ZHANG J X, LORIMER G W, ROBSON J. Review on research and development of magnesium alloys [J]. Acta Metallurgica Sinica (English Letters), 2008, 21(5): 313−328.

[2] ASHISH S, SANDIP P, HARIMKAR. Laser surface engineering of magnesium alloys: A review [J]. JOM, 2012, 64(6): 716−733.

[3] CUI Ze-qin, WU Hong-liang, WANG Wen-xian, XU Bing-she. Laser cladding Cu−Ni alloy layer on AZ31B magnesium alloy [J] The Chinese Journal of Nonferrous Metals, 2010, 20(9): 1665−1670. (in Chinese)

[4] BERNABE C, JESUS S, ANA R, XAVIER T. Corrosion and wear resistance improvement of magnesium alloys by laser cladding with Al−Si [J]. Physics Procedia, 2011, 12: 353−363.

[5] HAZRA M, MONDAL A K, KUMAR S, BLAWERT C, DAHOTRE N B. Laser surface cladding of MRI 153M magnesium alloy with ($Al+Al_2O_3$) [J]. Surface and Coatings Technology, 2009, 203(16): 2292−2299.

[6] QIAN Jian-gang, ZHANG Jia-xiang, LI Shu-qing, WANG Chun. Study on laser cladding $NiAl/Al_2O_3$ coating on magnesium alloy [J]. Rare Metal Materials and Engineering, 2013, 42(3): 466−469. (in Chinese)

[7] HUONG Kai-jin, YAN Li, WANG Cun-shan, XIE Chang-sheng, ZHOU Chang-rong. Wear and corrosion properties of laser cladded $Cu_{47}Ti_{34}Zr_{11}Ni_8$/SiC amorphous composite coatings on AZ91D magnesium alloy [J]. Transactions of Nonferrous Metals Society of China, 2010, 20(7): 1351−1355.

[8] NG C C, SAVALANI M M, MAN H C. Microstructure and mechanical properties of selective laser melted magnesium [J]. Applied Surface Science, 2011, 257(17): 7447−7454.

[9] TALTAVULL C, TORRES B, LOPEZ A J, RODRIGO P, RAMS J. Novel laser surface treatments on AZ91 magnesium alloy [J]. Surface & Coatings Technology, 2013, 222: 118−127.

[10] ZHANG S F, ZHANG R F, LI W K, LI M S, YANG G L. Effects of tannic acid on properties of anodic coatings obtained by micro arc oxidation on AZ91 magnesium alloy [J]. Surface & Coatings

Technology, 2012, 207: 170−176.

[11] GUO Hui-xia, MA Ying, WANG Jing-song, WANG Yu-shun, DONG Hai-rong, HAO Yuan. Corrosion behavior of micro-arc oxidation coating on AZ91D magnesium alloy in NaCl solutions with different concentration [J]. Transactions of Nonferrous Metals Society of China, 2012, 22(7): 1786−1793.

[12] SONG Ying-wei, SHAN Da-yong, CHEN Rong-shi, HAN En-hou. A novel dual nickel coating on AZ91D magnesium alloy [J]. Transactions of Nonferrous Metals Society of China, 2008, 18(S1): s339−s343.

[13] TAKAHIRO I, JUNKO H, NAGAHIRO S, NAOBUMI S, OSAMU T. Corrosion resistance and chemical stability of super-hydrophobic film deposited on magnesium alloy AZ31 by microwave plasma-enhanced chemical vapor deposition [J]. Electrochimica Acta, 2010, 55(23): 7094−7101.

[14] BARRANCO V, CARMONA N, GALVAN J C, GROBELNY M, KWIATKOWSKI L, VILLEGAS M A. Electrochemical study of tailored sol-gel thin films as pre-treatment prior to organic coating for AZ91 magnesium alloy [J]. Progress in Organic Coatings, 2010, 68(4): 347−355.

[15] JIN He-xi, WANG Ri-chu, PENG Chao-qun, FENG Yan, SHI Kai, CHEN Bin. Research progress of chemical conversion coatings on magnesium alloys [J]. The Chinese Journal of Nonferrous Metals, 2011, 21(9): 2049−2059. (in Chinese)

[16] YU Bing-long, LIN Jun-kai, WANG Jun-yan. Applications of carbonic acid solution for developing conversion coatings on Mg alloy [J]. Transactions of Nonferrous Metals Society of China, 2010, 20(7): 1331−1339.

[17] GAO Y, WANG C, YAO M, LIU H. Corrosion behavior of laser melted AZ91HP magnesium alloy [J]. Materials and Corrosion, 2007, 58(6): 463−466.

[18] GUAN Y C, ZHOU W, LI Z L, ZHENG H Y. Study on the solidification microstructure in AZ91D Mg alloy after laser surface melting [J]. Applied Surface Science, 2009, 255(19): 8235−8238.

[19] ABBAS G, LI L, GHAZANFAR U, LIU Z. Effect of high power diode laser surface melting on wear resistance of magnesium alloys [J]. Wear, 2006, 260(1−2): 175−180.

[20] COY A E, VIEJO F. Effect of excimer laser surface melting on the microstructure and corrosion performance of the die cast AZ91D magnesium alloy [J]. Corrosion Science, 2010, 52(2): 387−397.

[21] ZHANG Yong-kang, CHEN Ju-fang, LEI Wei-ning, XU Ren-jun. Effect of laser surface melting on friction and wear behavior of AM50 magnesium alloy [J]. Surface & Coatings Technology, 2008, 202(14): 3175−3179.

[22] XIE Guo-zhi, SONG Xiao-long. Microstructure and corrosion properties of thick WC composite coating formed by plasma cladding [J]. Applied Surface Science, 2010, 256(21): 6354−6358.

[23] CHEN Ju-fang, ZHANG Yong-kang, LI Ren-xing, QIN Hai-yong. Strengthening effect and mechanism of laser surface melted AM50A magnesium alloy [J]. The Chinese Journal of Nonferrous Metals, 2008, 18(8): 1426−1431. (in Chinese)

[24] VLADKOVA T G, KERANOV I L, DINEFF P D, YOUROUKOV S Y, AVRAMOVA I A, KRASTEVA N, ALTANKOV G P. Plasma based Ar^+ beam assisted poly (dimethyl siloxane) surface modification [J]. Nuclear Instruments and Methods in Physics Research Section B, 2005, 236(1−4): 552−562.

AZ91D 镁合金等离子束重熔组织与性能

崔洪芝，孟兆涛，肖成柱，孙金全，王翠香

山东科技大学 材料科学与工程学院，青岛 266590

摘　要：利用高能等离子束对 AZ91D 镁合金表面进行快速加热重熔处理，并对重熔层的显微组织、物相、硬度以及耐磨耐蚀性能进行分析。结果表明：在低放大倍数下，重熔层的组织为细小的枝晶，在高放大倍数下，晶粒为细小的等轴晶粒，尺寸为 5~7 μm；与基体相比，物相组成仍为 α-Mg 和 β-$Mg_{17}Al_{12}$，但 α-Mg 相减少，β-$Mg_{17}Al_{12}$ 增加，且 β-$Mg_{17}Al_{12}$ 相的分布更加均匀弥散；重熔层的显微硬度明显高于基体的显微硬度；重熔层拉伸断口与基体拉伸断口不同，有塑性变形痕迹以及由细小均匀韧窝组成的纤维状的撕裂痕，也有明显的晶粒拔出痕迹。等离子重熔处理提高了 AZ91D 镁合金的表面耐磨性和耐蚀性能。

关键词：镁合金；等离子重熔；固溶强化；细晶强化；耐磨性；耐蚀性

(Edited by Yun-bin HE)